

Double Drell-Yan annihilations in hadron collisions: Novel tests of the constituent picture

C. Goebel and D. M. Scott

Physics Department, University of Wisconsin at Madison, Madison, Wisconsin 53706

F. Halzen

*Physics Department, University of Hawaii at Manoa, Honolulu, Hawaii 96822
and Physics Department, University of Wisconsin at Madison, Madison, Wisconsin 53706*

(Received 26 December 1979; revised manuscript received 9 April 1980)

The production in hadron collisions of a pair of virtual photons, each having a large invariant mass, proceeds via two mechanisms: (a) two independent Drell-Yan-type annihilations of quark pairs in a single interaction and (b) the pair annihilation process $q\bar{q} \rightarrow \gamma^* \gamma^*$. We argue that both mechanisms allow intriguing tests of constituent structure and its associated scaling laws and we show that, despite their α^4 production rate, events of this type are accessible with existing π and proton beams.

The Drell-Yan process,¹ which describes the production of large mass lepton pairs in hadron interactions as due to the annihilation of quarks into virtual photons, has been a valuable testing ground for ideas regarding the properties and the dynamics (e.g., quantum chromodynamics) of hadron constituents. It is the purpose of this note to point out that observation of the process $pp \rightarrow \gamma^* \gamma^* X \rightarrow (4 \text{ leptons}) X$ probes the parton picture and its scaling properties in novel and penetrating ways.² We demonstrate that the process is observable with existing high-intensity π or proton beams, even though the cross section is of order α^4 .

Two competing mechanisms are responsible for producing two high-mass photons in a hadron collision. They are shown in Figs. 1(a) and 1(b) where the kinematics is defined. The first mechanism produces the photon pair via two Drell-Yan-type annihilations occurring in a single collision. The rate of this process clearly depends on the joint distribution $q(x, x')$ for finding two quarks with fractional momenta x, x' inside a hadron. Observation of this process could provide us with a first experimental glimpse at $q(x, x')$ which provides the computational basis for recombination-model³ calculations. The pair-annihilation process of Fig. 1(b), which as we will show closely competes in rate with the double annihilation of Fig. 1(a), allows the direct observation of a parton subprocess. Its observation would allow us to do two-jet physics, with an obvious experimental advantage: the jets are virtual photons. We now proceed to estimate the cross section for both processes. Introducing the notation (y is the center-of-mass rapidity)

$$\left(\frac{d\sigma}{dm dy} \right)_{y=0} \equiv \frac{d\sigma}{dm}$$

and

$$\left(\frac{d\sigma}{dm dy dm' dy'} \right)_{y=y'=0} = \frac{d\sigma}{dm dm'}$$

one can show that the double-annihilation cross section of Fig. 1(a) is given by

$$\frac{d\sigma/dm dm'}{(d\sigma/dm)(d\sigma/dm')} = \sum_{i,i'} \frac{e_i^2 e_{i'}^2}{\pi R^2} q(x_1, x_1') q(x_2, x_2') \quad (1)$$

with

$$\frac{d\sigma}{dm} = \frac{8\pi\alpha^2}{9} \frac{1}{ms} \quad (2)$$

where s is the c.m. energy squared. The summation is over quark types; e_i is the charge of the quark i . Since for illustrative purposes we have taken $y = y' = 0$,

$$x_1 = x_2 = \frac{m}{\sqrt{s}} \quad \text{and} \quad x_1' = x_2' = \frac{m'}{\sqrt{s}} \quad (3)$$

Equation (1) nicely displays the scaling properties of the process. The factor πR^2 in the denominator of Eq. (1) represents the hadronic total cross section, which is the estimate of the size of a hadron.⁴ The reason for this factor is that, given that one of the $q\bar{q}$ annihilations occurs, the probability of the other annihilation is proportional to the flux of accompanying quarks; these are confined to the hadrons, and their flux is thus inversely proportional to the area of a hadron. A more accurate estimate of this flux factor could be made only if the hadron structure were better known. (The cross section of an analogous process, the annihilation of a hydrogen atom on an antihydrogen atom, can be accurately calculated in the impulse approximation because one knows the atomic wave function, as well as the $p\bar{p}$ and e^-e^+ cross sections.) As an example of the possible large effects of structure effects, suppose that in a baryon two of the valence quarks are close together in space ("di-

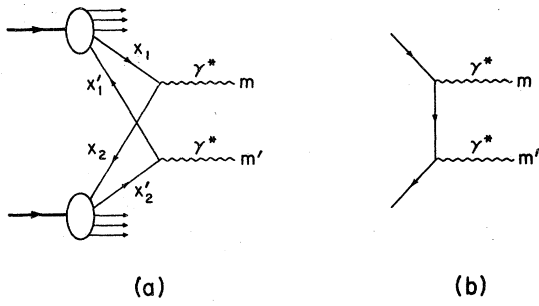


FIG. 1. Production of two high-mass virtual photons by (a) double and (b) single quark-antiquark annihilation.

quarks"; the string model suggests this). Then in $\frac{4}{9}$ of Drell-Yan $q\bar{q}$ annihilations in $p\bar{p}$ collisions both the q and the \bar{q} are members of a diquark and there is a large probability of a second annihilation, because of the small size of the diquarks.

The cross section for the process of Fig. 1(b) is given by

$$\frac{d\sigma}{dt} = \sum_i \frac{2\pi\alpha^2}{3} e_i^4 \frac{1}{s^2} \left[(tu - m^2 m'^2) \left(\frac{1}{t^2} + \frac{1}{u^2} \right) + 2s \left(\frac{m^2 + m'^2}{tu} \right) \right]. \quad (4)$$

s , t , u are the usual Mandelstam variables of the subprocess. Transformation to the frame of the colliding hadrons using quark structure functions is straightforward.

It is clear that only the appearance of the joint quark distributions $q(x, x')$ prevents us from routinely performing these calculations. But our ignorance of $q(x, x')$ does not prevent us from making a better than "order-of-magnitude estimate" of the rate, by the following argument. Let us denote by q_{vv} the joint distribution of two valence quarks in a hadron. Imposing the constraints that

$$q_{vv}(x, x') = q_{vv}(x', x), \quad (5)$$

$$\int_0^{(1-x)} dx' q_{vv}(x, x') = q_v(x) = a \frac{(1-x)^n}{\sqrt{x}}, \quad (6)$$

$$\int_0^1 dx q_v(x) = 1, \quad (7)$$

we obtain a definite result for $q(x, x')$ in the limit that hadrons are made up of (identical) valence quarks only. Taking n in Eq. (6) to be 1, 3 for a π meson and a nucleon, respectively, we have

$$q_{vv}^N(x, x') = \frac{7}{2\pi} \frac{(1-x-x')^{5/2}}{(xx')^{1/2}}, \quad (8)$$

$$q_{vv}^\pi(x, x') = \frac{3}{2\pi} \frac{(1-x-x')^{1/2}}{(xx')^{1/2}}. \quad (9)$$

At the valence-quark level Eq. (8) is sufficient

to determine the diagram of Fig. 1(a) in a $\bar{p}p$ interaction. However, πp and $p\bar{p}$ interactions involve the joint distribution of a valence and a sea quark in a nucleon. This distribution can be taken from phenomenological analyses using the recombination model,³ and probably an adequate guess is

$$q_{vs}^N(x, x') = a' q_v(x) q_s(x') (1-x-x'). \quad (10)$$

The factor $(1-x-x')$ is required by phase space. The constant a' can be inferred from the condition

$$\int_0^{1-x'} dx q_{vs}^N(x, x') = q_s(x'). \quad (11)$$

When using the valence-quark distributions of Eq. (6), Eq. (11) cannot be imposed exactly; we note, however, that $a' = \frac{9}{8}$ when x' approaches zero. This region should dominate the normalization requirement of Eq. (11).

We believe that these distributions allow us to make a reliable estimate of the cross sections. In $p\bar{p}$ interactions the calculation only involves q_{vv}^N and is therefore unambiguous at the valence-quark level, giving

$$\frac{d\sigma}{dn dn'} = \frac{1}{\pi R^2} \frac{d\sigma}{dn dn'} \rho(x_1, x_2, x'_1, x'_2), \quad (12)$$

where

$$\rho(x_1, x_2, x'_1, x'_2) = \sum_{i,i'} e_i^2 e_{i'}^2 q(x_1, x'_1) q(x_2, x'_2). \quad (13)$$

It is clear that for $m < m_\psi$ the process under consideration will be difficult to distinguish from pair production of resonances ρ, ϕ, ψ, \dots followed by two leptonic decays. Although observations of these processes would be very interesting, the physics involved is different and a straightforward perturbative estimate is difficult because of formidable problems such as how, for example, charmed quarks form colorless ψ 's. Avoiding the ψ region, let us choose $m = m' = 4$ GeV and $\sqrt{s} = 27$ GeV; therefore, $x_1 = x'_1 = x_2 = x'_2 = 0.15$. For $\bar{p}p$ interactions the structure function of Eq. (12) has the value $\rho \approx 10$, corresponding to a cross section of $10^{-16} - 10^{-15}$ mb/GeV. The low intensity of secondary \bar{p} beams makes observation difficult. One comes, however, to the opposite conclusion when considering high-intensity π or p beams. At the level of valence quarks inside a π meson,

$$\rho^{\pi N} = \left(\frac{2}{3}\right)^2 \left(\frac{1}{3}\right)^2 q_{vv}^\pi(x_1, x'_1) q_{vs}^N(x_2, x'_2). \quad (14)$$

A conservative estimate, neglecting all graphs involving sea quarks only, yields $\rho^{\pi N} \approx 0.1$ cor-

responding to a cross section of 10^{-17} mb/GeV. In $p\bar{p}$ interactions ρ is proportional to the square of ρ_{ψ}^N and is therefore suppressed; but the many combinatoric possibilities of valence quarks in one proton annihilating on sea quarks in the other make up for this effect yielding

$$\rho^{NN} \simeq 5\rho^{\pi N}, \quad (15)$$

consequently,

$$\rho^{NN} \simeq \frac{1}{10}\rho^{\bar{N}N}. \quad (16)$$

We therefore obtain a yield of about 5×10^{-17} mb/GeV for $p\bar{p}$ interactions.

The graph of Fig. 1(b) yields competitive cross sections. Again choosing $m=m'=4$ GeV, using standard technology for the structure functions, we obtain cross sections which are a factor 2–10 larger than our results quoted for the graph of Fig. 1(a). It is important to reiterate however that we evaluated the double-annihilation process of Fig. 1(a) in the limit that no more than one sea quark participates in the process. Processes involving two sea quarks are dynamically suppressed; there are so many of them, however, that they may add up to cross-section levels in excess of our previous calculation. Rough estimates, although not as straightforward or reliable as the computation of diagrams involving at least three valence quarks, show that this is indeed the case and in that sense the predictions of Eqs. (15) and (16) are not reliable. Conservative conclusions regarding tetralepton rates would be that both production mechanisms closely compete and yield cross sections for masses larger than m_ψ in excess of 10^{-16} mb/GeV, whatever the incident beam (see Table I).

These cross sections, though small, are accessible with present high intensity π and p beams. The Fermilab π -meson beam (5×10^9 particles per pulse with 6 pulses per minute) in a year of running on a tungsten target would be sensitive to cross sections at the level of 10^{-17} mb assuming an A^1 dependence of the cross section. In a nuclear-target experiment using the full proton beam, one could not only gain in cross section as discussed before, but a flux increase by factors 10^2 – 10^3 can be expected. For the combined production mechanisms our expectations therefore range from several (order 10) events in a πN to order 10^3 events in an NN experiment.

In judging the relative merits of different beam particle types, one should also consider the problem of accidental coincidences of two single Drell-Yan events occurring within the time resolution of the detector and not resolvable in space after reconstruction. To a number of

double Drell-Yan events

$$N = \frac{\sigma_2}{\sigma} N_t t \quad (17)$$

corresponds a background-to-signal ratio (B/S) due to accidental overlap of two conventional Drell-Yan events:

$$(B/S) = \frac{\sigma_1^2}{\sigma\sigma_2} N_t \Delta t \frac{1}{\nu}. \quad (18)$$

Here we introduced the following notation: σ_1 (σ_2) cross section for single (double) Drell-Yan events, σ total interaction cross section, N_t number of beam particles on target per second, t total running time, Δt time resolution, and ν number of resolved spatial elements in the interaction region of the target. If one can resolve λ_a/n longitudinal distance, where λ_a is the absorption length, or the target is segmented in n pieces per absorption length, then $\nu \simeq n$. It is reasonable to assume $n \simeq 10$; therefore, $1/\nu \simeq 0.1$; a more careful calculation yields $1/\nu = 0.05$. The resulting calculation of (B/S) is shown in Fig. 2 for proton-induced interactions. In agreement with our previous estimates, we have assumed that both mechanisms contribute about equally to σ_2 . The diagram of Fig. 1(b) almost certainly depends on A as A^1 . As the quarks in the diagram of Fig. 1(a) can come from different nucleons, the dependence is somewhere between $A^{4/3}$ and A^2 . It is worthwhile to notice that by using targets with multiple nuclear composition, one can unambiguously separate the two production mechanisms experimentally. The numbers for π beams are very similar to those shown in Fig. 2. The results for the \bar{p} case can be directly obtained from those obtained for proton-induced interactions by combining Eqs. (12), (17), and (18) and noticing that $\sigma = \pi R^2$,

$$\frac{N\bar{p}}{Np} = \frac{\rho^{\bar{N}N}}{\rho^{NN}} \simeq 10,$$

and

$$\frac{(B/S)\bar{p}}{(B/S)p} = \frac{\rho^{NN}}{\rho^{\bar{N}N}} \simeq 10^{-1}. \quad (19)$$

TABLE I. Summary of rates on a hydrogen target, for $m=m'=4$ GeV and incident energy $\sqrt{s}=27$ GeV. Cross sections are in mb/GeV².

Beam-particle type	Diagram of Fig. 1(a)	Diagram of Fig. 1(b)
\bar{p}	$> 10^{-15}$	4×10^{-15}
π	$> 10^{-17}$	3×10^{-16}
p	$> 5 \times 10^{-17}$	2×10^{-16}

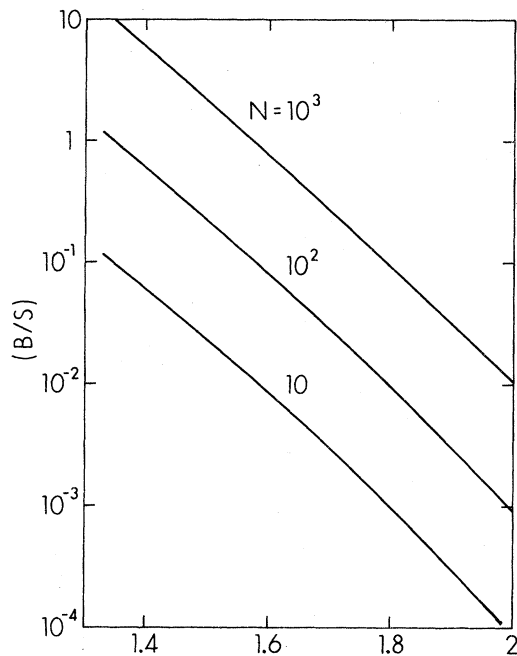


FIG. 2. Background-to-signal ratio from coincidences of single Drell-Yan events as a function of α , parametrizing the A^α nuclear dependence of the process of Fig. 1(a). N is the number of events per year. We assumed Eqs. (17) and (18) with $A \approx 200$, $\Delta t \approx 10^{-8}$ sec, and $1/\nu \approx 0.05$ corresponding to a spatial resolution of $\frac{1}{10}$ of an absorption length.

Inspecting Fig. 1, one sees that the accidental rates are quite tolerable.

Present experiments and beam intensities can expect rates of 10^2 – 10^3 per year. With a little help of the A dependence spatial separation of

the events is not even required.

We conclude that observation of double Drell-Yan events could allow us to study (i) combined scaling behavior in the three variables m , m' , and \sqrt{s} , (ii) parton cross sections without the necessity of identifying jets in the final state, (iii) the effective rms of quarks inside a hadron, and (iv) possible correlations between nucleons in nuclei. We also conclude that observation of tetralepton events is possible in present direct lepton experiments, whether they are using conventional proton or high-intensity π -meson beams. Although the experimental signature of these events would fit into the gold-plated category, the leptonic decay of π 's separated in angle and rapidity could fake large invariant masses. Observation in the $e^+e^-\mu^+\mu^-$ mode would be preferable. This is strictly speaking what we computed in Eq. (4) for the graph of Fig. 1(b), since we neglected exchange; i.e., alternative ways of pairing the leptons. The effect is not going to qualitatively alter our conclusions and will in fact depend on the coverage of the experiment.

ACKNOWLEDGMENTS

We thank B. Cox and B. Pope for encouragement. This research was supported in part by the University of Wisconsin Research Committee with funds granted by the Wisconsin Alumni Research Foundation, and in part by the Department of Energy under Contracts Nos. DE-AC02-76ER00881, C00-881-125, and DE-AC03-76ER00511.

¹S. D. Drell and T.-M. Yan, Phys. Rev. Lett. **25**, 316 (1970); Ann. Phys. (N.Y.) **66**, 578 (1971).

²The potential importance of this process was repeatedly emphasized to us by D. Cline and D. Winn.

³For recent reviews, see R. C. Hwa, in *Proceedings of the IX International Symposium on High Energy Multi-particle Dynamics, Tábov, Czechoslovakia, 1978*

(Czechoslovak Academy of Science, Institute of Physics, Prague, 1978); L. Van Hove, Schladming lecture 1979, Report No. TH. 2628-CERN (unpublished).

⁴Multiple-scattering cross sections have been normalized in a similar way by A. Donnachie and P. V. Landshoff, Z. Phys. C **2**, 55 (1979).